

No-Reference Stereoscopic Video Quality Assessment Using Joint Motion and Depth Statistics

Balasubramanyam Appina, Akshith Jalli, Shanmukha Srinivas Battula, Sumohana S. Channappayya

Abstract—We present a no-reference (NR) quality assessment algorithm for assessing the perceptual quality of natural stereoscopic 3D (S3D) videos. This work is inspired by our finding that the joint statistics of the subband coefficients of motion (optical flow or motion vector magnitude) and depth (disparity map) of natural S3D videos possess a unique signature. Specifically, we empirically show that the joint statistics of the motion and depth subband coefficients of S3D video frames can be modeled accurately using a Bivariate Generalized Gaussian Distribution (BGGD). We then demonstrate that the parameters of the BGGD model possess the ability to discern quality variations in S3D videos. Therefore, the BGGD model parameters are employed as motion and depth quality features. In addition to these features, we rely on a frame-level spatial quality feature that is computed using a robust off-the-shelf NR image quality assessment (IQA) algorithm. These frame-level motion, depth and spatial features are consolidated and used with the corresponding S3D video's difference mean opinion score (DMOS) labels for supervised learning using support vector regression (SVR). The overall quality of an S3D video is computed by averaging the frame-level quality predictions of the constituent video frames. The proposed algorithm, dubbed Video Quality Evaluation using MOtion and DEpth Statistics (VQUEMODES) is shown to outperform the state-of-the-art methods when evaluated over the IRCCYN and LFOVIA S3D subjective quality assessment databases.

Index Terms—Stereoscopic video, No-reference quality assessment, BGGD, Depth and Motion.

I. INTRODUCTION

The advancements in digital multimedia technologies over the past decade have received tremendous consumer acceptance. Stereoscopic 3D (S3D) digital technology has received a lot of attention lately and several industries such as film, gaming, education etc., are focused on S3D content creation. The Motion Pictures Association of America MPAA [1] and Statista [2] reported that in 2015, the S3D movie box office profit reached \$1.7 billion and this was an increase of 20% compared to 2014. They also reported that the number of S3D screens in 2015 increased by 15% compared to 2014 in the United States (US). These numbers are a clear indication of the advancements in S3D technology and its ever increasing popularity with consumers.

S3D video content creation [3] involves several processing steps like sampling, quantization, synthesis etc. Each step in this processing chain affects the perceptual quality of the source video content leading to a degradation of the Quality of Experience (QoE) of the end user. To guarantee high

user satisfaction, it becomes important to assess the loss in quality at each step of the lossy process. Quality assessment (QA) is the process of judging or estimating the quality of a video according to its perceptual experience. QA can be categorized into two types: subjective and objective. In subjective assessment, the viewers quantify their opinion on video quality based on their perceptual feel after viewing the content. Objective quality assessment refers to the automatic quality evaluation process designed to mimic subjective assessment. It has three flavors: full reference (FR) where the pristine source is available for QA, reduced reference (RR) where partial information about the pristine source is available for QA and no-reference (NR), where no pristine source information is available for QA. In this work, we focus on S3D NR video quality assessment (VQA).

The predominant approach to objectively assessing the quality of S3D content (image and video) has been to leverage the strength of 2D QA algorithms in conjunction with a factor that accounts for depth quality (for e.g., [4]–[11]). The reliance on 2D QA metrics for S3D quality assessment could be explained by the fact that depth perception is a consequence of the relative spatial shift present in two 2D images. Another reason for relying on 2D QA methods could be the fact that they are far more mature given the ubiquity of 2D content. Further, access to publicly available S3D subjective quality databases is very limited in general, and even more so in the case of videos. In contrast to the 2D QA reliant approach, we propose an NR S3D VQA algorithm based on statistical properties that are *innately stereoscopic* and lightly augment it with a 2D NR spatial score. Towards this end, we propose a joint statistical model of the multi scale subband coefficients of motion and depth components of a natural S3D video sequence. Specifically, we propose a Bivariate Generalized Gaussian Distribution (BGGD) model for this joint distribution. We show that the BGGD model parameters possess good distortion discrimination properties. The model parameters combined with frame-wise 2D NR spatial quality scores are used as features to train an SVR for the NR VQA task.

The rest of the paper is organized as follows: Section II reviews relevant literature. Section III presents the proposed joint statistical model and the NR S3D VQA algorithm. Section IV presents and discusses the results of the proposed NR VQA algorithm. Concluding remarks are made in Section V.

The authors are with the Lab for Video and Image Analysis (LFOVIA), Department of Electrical Engineering, Indian Institute of Technology Hyderabad, Kandi, India, 502285 e-mail: {ee13m14p100001, ee13b1013, ee13b1006, sumohana}@iith.ac.in.

II. BACKGROUND

Given that our contribution spans S3D video modeling and VQA, we review relevant literature in appropriately titled subsections in the following.

A. Motion and Depth Dependencies in the Human Visual System (HVS)

Maunsell and Van Essen [12] performed psychovisual experiments on the monkey visual cortex to explore the disparity selectivity in the middle temporal (MT) visual area. They found that two-thirds of MT area neurons are highly tuned and responsible for binocular disparity processing. Roy *et al.* [13] experimented on a large number of MT area neurons (295 neurons) of awake monkeys to explore the dependencies between motion and depth components. They concluded that 95% of the tested neurons were highly responsive to the crossed and uncrossed disparities. De Angelis and Newsome [14] performed psychovisual experiments to explore the depth tuning in the MT area. They concluded that the MT neurons are primarily responsible for motion perception and also that these neurons are important for depth perception. Dayan *et al.* [15] performed an experiment on the MT area of Macaque monkeys to model the firing response rate of a neuron. They hypothesized that the frequency response of neuron firing rate can be accurately modeled with a generalized gaussian distribution. These findings combined with the observation that neuronal responses are tuned to the statistical properties of the sensory input or stimuli [16] motivate us to study and model the joint statistical relationship between the subband coefficients of motion and depth components of the *stimuli* i.e., natural S3D videos.

B. S3D Natural Scene Statistical Modeling

We briefly review literature on S3D natural scene statistical modeling. Huang *et al.* [17] explored the range statistics of a natural S3D scene. The range maps are captured using laser range finder and pixel, gradient and wavelet statistics are modeled. Liu *et al.* [18], [19] computed the disparity information from the depth maps which were created using range finders. They established a spherically modeled eye structure to construct the disparity maps and finally correlated the constructed disparity maps with stereopsis of HVS maps. Potetz and Lee [20] and Liu *et al.* [21], [22] studied the statistical relationship between the luminance and spatial disparity maps in a multiscale subband decomposition domain. They concluded that the histograms of luminance and range/disparity subband coefficients have sharp peaks and heavy tails and can be modeled with a univariate GGD (UGGD). Further, they explored the correlation dependencies between these subband coefficients. Su *et al.* [23] performed a study to explore the relationship between chrominance and range components. They found that the conditional distribution of chrominance coefficients (given range gradients) is modeled well using a Weibull distribution. While these studies focused on static S3D natural scenes, we found few studies on the joint statistics of motion and depth components of S3D natural

videos. This paucity has provided additional motivation for our work.

C. S3D Video Quality Assessment

We now review S3D video quality assessment methods in the following. These methods could broadly be classified into statistical modeling based and human visual system (HVS) based approaches.

Statistical model based approaches have been very successful in S3D IQA [24]–[28]. Mittal *et al.* [29] proposed an NR S3D VQA metric based on statistical measurements of disparity and differential disparity. They computed the mean, median, kurtosis, skew-ness and standard deviation values of the disparity and differential disparity maps to estimate the quality of an S3D video. These approaches point to the efficacy of using statistical models for S3D QA, and provide the grounding for our work.

As discussed earlier, several objective S3D FR VQA models [4]–[10] are based on applying 2D IQA/VQA algorithms on individual views and the depth component of an S3D video. In addition to these, we review a few HVS inspired FR, RR and NR VQA algorithms next. [30] and [31] proposed S3D VQA models based on 3D-Discrete Cosine Transform (DCT) and 3D structure models from the spatial, temporal and depth components of an S3D view. Qi *et al.* [32] proposed an FR S3D VQA metric based on measuring the Just Noticeable Differences (JND) on spatial, temporal and depth maps. They computed the temporal JNDs (TJND) of spatial component and interview JNDs (IJND) from TJNDs to estimate the binocular property. Further, they calculated the similarity maps between reference and distorted spatial JNDs to estimate the spatial quality and finally, they computed the mean across all JNDs to estimate the overall S3D video quality score. De Silva *et al.* [33] proposed an FR S3D VQA metric based on measuring the perceivable distortion strength from depth maps. They computed the JND value between reference and distorted depth maps to measure the quality of an S3D video. Galkandage *et al.* [34] proposed S3D FR IQA and VQA metrics based on an HVS model and temporal features. They computed the Energy Quality Metric (EBEQM) scores to measure the spatial quality and finally pooled these scores by using empirical methods to estimate the overall quality score of an S3D video. De Silva *et al.* [35] proposed an S3D FR VQA based on measuring the spatial distortion, blur measurement and content complexity. They measured the structural similarity and edge degradation between reference and distorted views to compute the spatial quality, distortion strength. Content complexity was measured by calculating the spatial and temporal indices of an S3D view.

Hewage and Martini *et al.* [36] proposed an S3D RR VQA metric based on depth map edges and S3D view chrominance information. They applied the Sobel operator to compute the edges of a depth map and utilized these edges to extract the chrominance features of an S3D view. Finally, they computed the PSNR values of extracted features to estimate the quality of an S3D video. Yu *et al.* [37] proposed an S3D RR VQA metric based on perceptual properties of the HVS. They relied on motion vector strength to predict the reduced reference frame

of a reference video, and binocular fusion and rivalry scores were calculated using the RR frames. Finally these scores were pooled using motion intensities as weights to compute the quality score of an S3D video.

Sazzad *et al.* [38] proposed an S3D NR VQA metric based on spatiotemporal segmentation. They measured structural loss by computing the edge strength degradation in each segment and motion vector length was measured to estimate the temporal cue loss. Ha and Kim [39] proposed an S3D NR VQA metric based on temporal variance, intra and inter disparity measurements. Depth maps are computed by minimizing the MSE values, and motion vector length is calculated to estimate the temporal variations. Intra and inter frame disparities were computed to measure the dependencies between motion and depth components. Solh and AlRegib [40] proposed an S3D NR VQA metric based on temporal inconsistencies, spatial and temporal outliers. Spatial and temporal outliers were measured by calculating the difference between ideal and estimated depth maps, and temporal inconsistencies were computed by calculating the standard deviation of difference between depth maps of successive frames. Hasan *et al.* [41] proposed an S3D NR VQA metric based on similarity matches and edge visualized areas. They utilized the edge strength to find the visualized areas and computed the energy error of similarity measure estimated between left and right views to calculate the disparity index. Silva *et al.* [42] proposed an S3D NR VQA metric based on distortion strength, disparity and temporal depth qualities of a 3D video. They computed the depth cue loss by measuring the spatial distortion strength, and temporal depth qualities were measured by calculating the correlation between histograms of frame motion vectors. Han *et al.* [43] proposed an NR S3D VQA metric based on the encoder settings of a transmitted video. They used the ITU-T G.1070 settings to model the packet loss artefacts and quality was measured by computing the correlation between perceptual scores and packet loss rates at different bit rates. Mahmood and Ghani [44] proposed an S3D NR VQA metric based on computing the motion vector lengths and depth map features. They concluded that the number of bad frames in a video is a good predictor of motion and depth quality of an S3D video. Yang *et al.* [45] proposed an S3D NR VQA metric based on multi view binocular perception model. They applied the curvelet transform on spatial information of an S3D video to extract the texture analysis features and optical flow features were utilized to measure the temporal quality. Finally, they used empirical weight combinations to pool these scores to compute the overall quality score. Chen *et al.* [46] proposed an S3D NR VQA model based on binocular energy mechanism. They computed the auto-regressive prediction based disparity measurement and natural scene statistics of an S3D video to compute the quality.

Our literature survey has equipped us with the required background and motivation to study and model the joint statistics of motion and depth in S3D natural videos in a multi-resolution analysis domain. Further, it has given us the grounding to propose an S3D NR VQA algorithm dubbed Video Quality Evaluation using MOtion and DEpth Statistics (VQUEMODES) that relies on the joint statistical model

parameters and 2D NR IQA scores. We describe the proposed approach in detail in the following section.

III. PROPOSED METHOD

We first analyze the joint statistical behavior of the subband coefficients of motion and depth components in S3D natural videos. We then propose a BGGD model for the joint distribution. Subsequently, we describe the proposed S3D NR VQA algorithm.

A. BGGD Modeling

We empirically show that a Bivariate Generalized Gaussian Distribution (BGGD) accurately captures the dependencies between motion and depth subband coefficients. We use both optical flow vector magnitude and motion vector magnitude to represent motion in our statistical analysis. We do so to investigate the behavior at both fine and coarse motion representations respectively. Further, motion vector computation has significantly lower computational complexity compared to optical flow computation. We perform our analysis using multi-scale (3 scales) and multi-orientation ($0^0, 30^0, 60^0, 90^0, 120^0, 150^0$) subband decomposition coefficients of the motion (optical flow/motion vector) and disparity maps.

The multivariate GGD distribution of a random vector $\mathbf{x} \in \mathbb{R}^N$ is given by [47]

$$p(\mathbf{x}|\mathbf{M}, \alpha, \beta) = \frac{1}{|\mathbf{M}|^{\frac{1}{2}}} g_{\alpha, \beta}(\mathbf{x}^T \mathbf{M}^{-1} \mathbf{x}), \quad (1)$$

$$g_{\alpha, \beta}(y) = \frac{\beta \Gamma(\frac{N}{2})}{(2^{\frac{1}{\beta}} \Pi \alpha)^{\frac{N}{2}} \Gamma(\frac{N}{2\beta})} e^{-\frac{1}{2}(\frac{y}{\alpha})^{\beta}}, \quad (2)$$

where \mathbf{M} is an $N \times N$ symmetric scatter matrix, β is the shape parameter, α is the scale parameter and $g_{\alpha, \beta}(\cdot)$ is the density generator.

Figs. 1(a) and 1(c) show the first and second frames of the Boxers S3D video left view respectively, and Fig. 1(b) shows the first frame of the right view from the Boxers video sequence of the IRCCYN database [48]. Fig. 1(f) shows the disparity map estimated using the SSIM-based stereo matching algorithm [49] computed between first frame of left and right views. Figs. 1(d) and 1(e) show the optical flow and motion vector maps computed between the first and second frames of the left view respectively. The optical flow map is computed using the Black and Anandan [50] flow algorithm and the motion vector map is estimated using the three-step block motion estimation algorithm [51]. Figs. 1(i), 1(g) and 1(h) show the histograms of the subband coefficients of disparity, optical flow magnitude and motion vector magnitude respectively. Fig. 1(j) shows the joint histogram between disparity and optical flow magnitude subband coefficients, and Fig. 1(l) shows the estimated BGGD model of 1(j). Fig. 1(k) shows the joint histogram of disparity and motion vector magnitude subband coefficients and Fig. 1(m) shows the estimated BGGD model of 1(k). The BGGD model parameters were estimated using the approach taken by Su *et al.* [26]. The marginal and joint histogram plots were computed at the first scale and 0^0 orientation of the steerable pyramid decomposition. From



(a) Reference left view first frame.



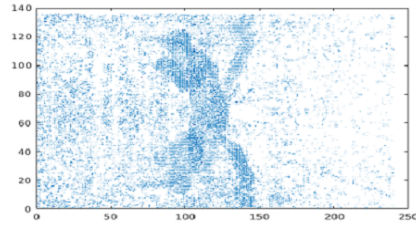
(b) Reference right view first frame.



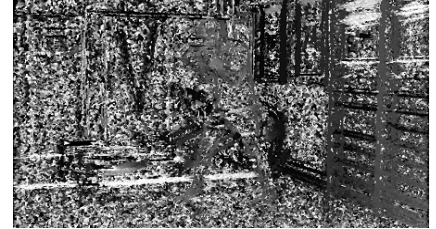
(c) Reference left view second frame.



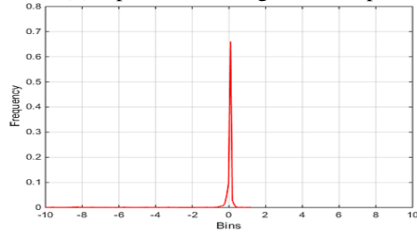
(d) Optical flow magnitude map.



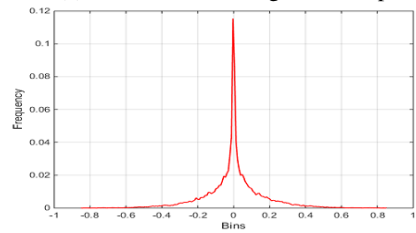
(e) Motion vector magnitude map.



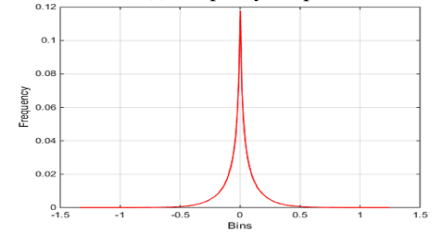
(f) Disparity map.



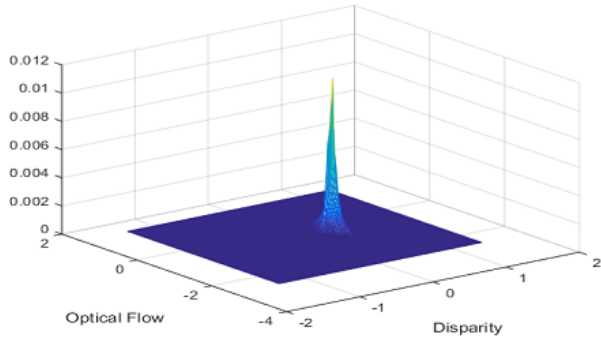
(g) Optical flow magnitude histogram.



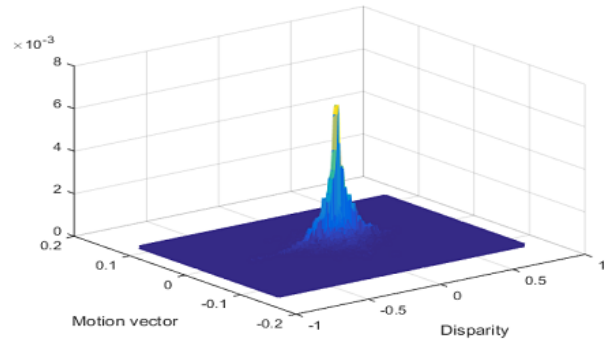
(h) Motion vector magnitude histogram.



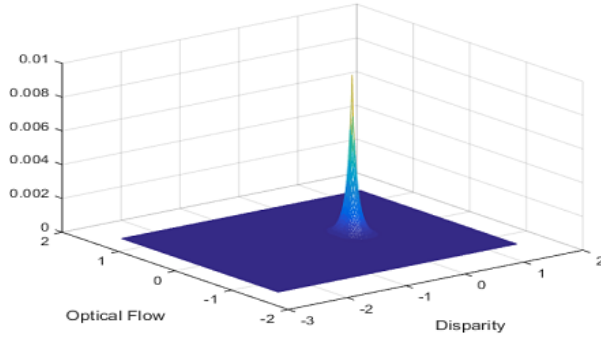
(i) Disparity map histogram.



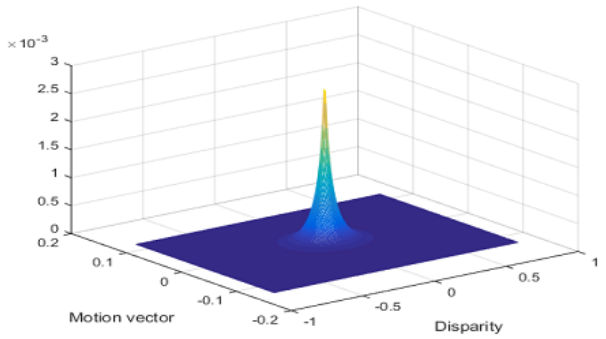
(j) Joint histogram plot of optical flow magnitude and disparity maps.



(k) Joint histogram plot of motion vector magnitude and disparity maps.



(l) Bivariate GGD fit between optical flow magnitude and disparity maps.



(m) Bivariate GGD fit between motion vector magnitude and disparity maps.

Fig. 1: Illustration of BGGD model fit between combinations of optical flow magnitude and disparity maps, motion vector magnitude and disparity maps.

the histograms 1(i), 1(g) and 1(h) we see that the subband coefficients have sharp peaks and long tails and is consistent with the observations in [15], [52]. The joint histograms between disparity and motion components 1(l) and 1(m) also have sharp peaks and heavy tails. These empirical findings lead us to propose that a bivariate GGD ($N = 2$) is ideally suited to model the joint distribution of disparity and motion subband coefficients.

The efficacy of the proposed BGGD model is first evaluated on three publicly available S3D video databases: IRCCYN [48], RMIT [53] and LFOVIA [54]. The IRCCYN video database has pristine S3D videos and their H.264 and JP2K distorted versions, the RMIT database comprises pristine S3D videos and the LFOVIA database is composed of pristine S3D videos and their H.264 compressed versions. Table I shows the estimated BGGD model fitting parameters between disparity and motion (optical flow and motion vector) subband coefficients of the 100th frame of a few reference S3D video sequences and their symmetric distortion combinations of the IRCCYN, LFOVIA and RMIT databases. The results are computed at the first scale and 0^0 orientation of the steerable pyramid decomposition. (α_o, β_o) correspond to optical flow parameters and (α_m, β_m) correspond to motion vector parameters. χ indicates the goodness of fit value and it represents how well the proposed model fits our observations (joint histogram). The low values of the χ point to the accuracy of the proposed model. χ_o is the goodness of fit value computed for the optical flow case. Similarly, χ_m is goodness of fit value for the motion vector case. In our analysis we observed that χ_o, χ_m are in the range 10^{-8} and 10^{-6} for all S3D video sequences. From these results it is clear that the proposed BGGD model performs well in capturing the joint statistical dependencies between motion and disparity subband coefficients.

B. Distortion Discrimination

Since we are interested in NR VQA of S3D videos, we explored the efficacy of the proposed model on distorted videos as well. Fig. 2(a) shows the first frame of left reference view, and Figs. 2(b) and 2(c) show the first frame of H.264 and JP2K distorted videos of corresponding reference view respectively. Due to a lack of other distortion types in the publicly available S3D video databases, we limited our analysis to H.264 and JP2K distortions. Figs. 2(d), 2(e) and 2(f) show the isoprobability contour plots of the joint optical flow magnitude and disparity subband coefficient distribution of the reference, H.264 and JP2K distorted frames respectively. These plots are computed at the first scale and 0^0 orientation of the steerable pyramid decomposition. The plots clearly show the strong dependencies between motion and depth components of an S3D view and further, the variation in the dependencies due to distortion. As a consequence, the effects of distortion manifest themselves in a change in the BGGD model parameters. Further, it can also be seen that H.264 and JP2K distortions result in distributions with heavier tails. We observed the same trend in the joint motion vector magnitude and disparity subband coefficients distributions.

Figs. 2(g), 2(h) and 2(i) show the isoprobability contour plots of the joint motion vector magnitude and disparity subband coefficient distribution of the reference, H264 and JP2K distorted frames respectively. As with optical flow, these plots correspond to the subband coefficients at the first scale and 0^0 orientation of the steerable pyramid decomposition. Again, we see a similar distortion tracking trend with the corresponding BGGD model parameters. Fig. 3 shows the distribution of BGGD coefficients (α_m, β_m) computed at the first scale and 0^0 orientation of all frames of the reference Boxers video and its H.264 distorted sequences at different QP (QP = 32, 38, 44) levels. It is clear that the BGGD features are able to discriminate the quality variations in S3D videos. As mentioned earlier, we consider motion vector magnitude in our work primarily due to their amenability for fast implementations. From Figs. 2 and 3, we have demonstrated that they have very good distortion discrimination properties as well.

C. Video Quality Algorithm

The flowchart of the proposed algorithm is shown in Fig. 4. The feature extraction stage estimates frame-wise BGGD model parameters to represent motion and depth quality features, and relies on the average 2D NR IQA score as the spatial quality feature. These features are then used to train an SVR for frame-wise quality scores. For video-level quality prediction, the individual frame-wise quality predictions are simply averaged. The algorithm is described in detail in the following.

D. Feature Extraction

1) *Motion Vector Estimation*: The temporal (motion) features are extracted using motion vectors. The motivation to use motion vectors is based on our observations in the previous section that they are as effective as optical flow in distortion discrimination. Also, motion vector computation takes a fraction of the cost of computing the optical flow vectors. We used the three-step search method [51] to estimate the motion vectors between successive frames and employed a macroblock size of 8×8 . Further, the magnitude of the motion vector is used to compute the temporal feature in our algorithm.

$$M_s = \sqrt{M_H^2 + M_V^2},$$

where, M_s represents the motion vector strength, M_H and M_V are horizontal and vertical motion vector components. Several video quality models [39], [55] have effectively used motion vectors as temporal features in their work.

2) *Disparity Estimation*: The human visual system takes two retinal views as input and fuses them into a single scene point by converting the scene differences of the two views into disparity/depth information. The simple and complex cells extract the structural properties of both views (spatial and temporal) and further, this information is processed in the primary visual cortex to construct a single scene point illusion of depth perception [56], [57]. In our work, the disparity maps are computed using an SSIM-based stereo-matching algorithm [49] for a given stereoscopic frame pair at every time instant.



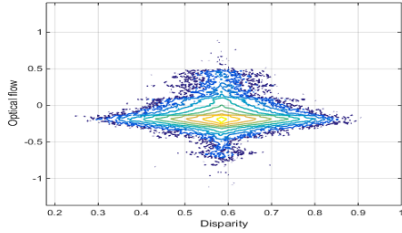
(a) Reference left view.



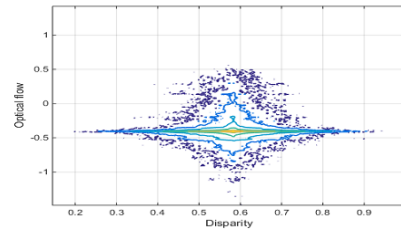
(b) H.264 compressed left view.



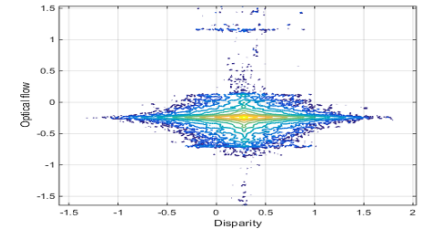
(c) JP2K distorted left view.



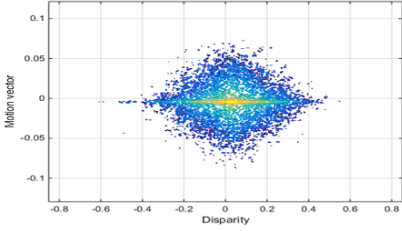
(d) Isoprobability contour plot of joint optical flow magnitude and disparity distribution of the reference view. Best fit BGGD model: $\alpha_o = 5 \times 10^{-14}$, $\beta_o = 0.0405$, $\chi_o = 1 \times 10^{-7}$.



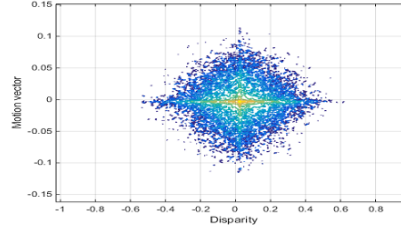
(e) Isoprobability contour plot of joint optical flow magnitude and disparity distribution of the H.264 distorted view. Best fit BGGD model: $\alpha_o = 1 \times 10^{-8}$, $\beta_o = 0.0514$, $\chi_o = 1 \times 10^{-8}$.



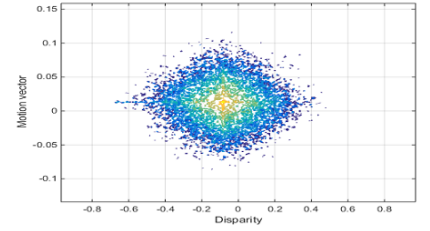
(f) Isoprobability contour plot of joint optical flow magnitude and disparity distribution of the JP2K distorted view. Best fit BGGD model: $\alpha_o = 1 \times 10^{-16}$, $\beta_o = 0.4238$, $\chi_o = 5 \times 10^{-7}$.



(g) Isoprobability contour plot of joint motion vector magnitude and disparity distribution of reference view. Best fit BGGD model: $\alpha_m = 4 \times 10^{-5}$, $\beta_m = 0.3579$, $\chi_m = 1 \times 10^{-8}$.



(h) Isoprobability contour plot of joint motion vector magnitude and disparity distribution of H.264 distorted view. Best fit BGGD model: $\alpha_m = 4 \times 10^{-4}$, $\beta_m = 0.4457$, $\chi_m = 8 \times 10^{-7}$.



(i) Isoprobability contour plot of joint motion vector magnitude and disparity distribution of JP2K distorted view. Best fit BGGD model: $\alpha_m = 6 \times 10^{-7}$, $\beta_m = 0.603$, $\chi_m = 6 \times 10^{-7}$.

Fig. 2: Effects of distortion on the joint distribution of motion and depth subband coefficients (0^0 orientation and first scale). It can be seen that the BGGD model parameters are able to track the effects of distortions.

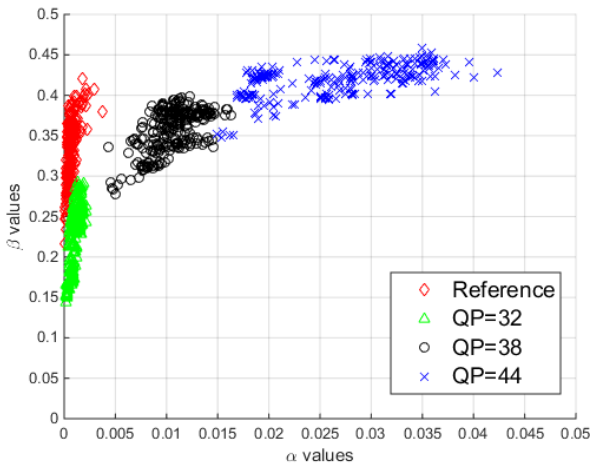







Fig. 3: BGGD model parameter variation of reference and H.264 distortion levels of the Boxers video sequence of IRCCYN S3D database. Each point in the scatter plot represents the model parameter pair (α_m, β_m) for a frame-pair in the corresponding video. The (α_m, β_m) pair clearly discriminate varying quality levels.

This algorithm works on the principle of finding the best matching block in the right view of a specific block in the corresponding left view. We chose this algorithm based on a trade-off between accuracy and time complexity. Since the temporal features are computed at a block size of 8×8 , we downsampled the disparity map subbands to the same size by averaging over an 8×8 block.

3) *Motion and Depth Feature Extraction:* Once the motion vector map and disparity map is computed for every frame, the BGGD model parameters are estimated using the joint histogram of the subband coefficients of the motion vector magnitude and the disparity map. As mentioned earlier, we rely on the method in [26] for parameter estimation. Specifically, these are computed at three scales and six orientations ($0^0, 30^0, 60^0, 90^0, 120^0, 150^0$) of the steerable pyramid decomposition.

4) *Spatial Feature Extraction:* The third feature we employ in our algorithm is the spatial quality of the video. Spatial quality is computed on a frame-by-frame basis by averaging

TABLE I: BGGD features (α , β) and goodness of fit (χ) value of reference S3D videos and its symmetric distortion combinations of IRCCYN, LFOVIA and RMIT databases.

Video Frame	Distortion Type	Test stimuli		BGGD features (α , β) and goodness of fit (χ) value					
		Left	Right	α_o	β_o	χ_o	α_m	β_m	χ_m
	Reference	-	-	1×10^{-5}	0.337	3×10^{-6}	8×10^{-6}	0.312	2×10^{-6}
	H.264 (QP)	32	32	2×10^{-6}	0.213	7×10^{-6}	6×10^{-7}	0.245	5×10^{-6}
		38	38	3×10^{-5}	0.341	3×10^{-6}	8×10^{-5}	0.377	2×10^{-6}
		44	44	1×10^{-4}	0.407	2×10^{-6}	7×10^{-4}	0.425	1×10^{-6}
	JP2K (Bitrate = Mb/s)	2	2	3×10^{-4}	0.715	1×10^{-6}	4×10^{-6}	0.737	1×10^{-7}
		8	8	1×10^{-4}	0.698	2×10^{-7}	3×10^{-5}	0.724	2×10^{-7}
		16	16	1×10^{-5}	0.619	4×10^{-7}	4×10^{-4}	0.641	3×10^{-7}
	Reference	-	-	3×10^{-11}	0.652	2×10^{-7}	5×10^{-4}	0.496	2×10^{-7}
	H.264 (QP)	32	32	6×10^{-6}	0.284	3×10^{-7}	5×10^{-5}	0.349	1×10^{-6}
		38	38	1×10^{-4}	0.372	2×10^{-6}	1×10^{-4}	0.395	1×10^{-6}
		44	44	2×10^{-4}	0.405	1×10^{-6}	3×10^{-4}	0.441	9×10^{-7}
	JP2K (Bitrate = Mb/s)	2	2	1×10^{-11}	0.622	2×10^{-7}	2×10^{-9}	0.649	2×10^{-7}
		8	8	1×10^{-11}	0.677	2×10^{-7}	2×10^{-10}	0.611	2×10^{-7}
		16	16	4×10^{-11}	0.585	2×10^{-7}	6×10^{-10}	0.600	2×10^{-7}
	Reference	-	-	5×10^{-5}	0.361	7×10^{-7}	5×10^{-5}	0.361	7×10^{-7}
	H.264 (Bitrate=Kbps)	100	100	2×10^{-6}	0.318	3×10^{-6}	7×10^{-5}	0.365	1×10^{-6}
		200	200	2×10^{-5}	0.447	8×10^{-7}	3×10^{-6}	0.281	4×10^{-6}
		350	350	9×10^{-5}	0.435	5×10^{-7}	2×10^{-6}	0.268	3×10^{-6}
		1200	1200	2×10^{-4}	0.438	3×10^{-7}	2×10^{-5}	0.332	1×10^{-6}
	Reference	-	-	1×10^{-4}	0.205	9×10^{-6}	2×10^{-7}	0.230	5×10^{-6}
	H.264 (Bitrate=Kbps)	100	100	9×10^{-5}	0.430	3×10^{-6}	4×10^{-4}	0.449	1×10^{-6}
		200	200	3×10^{-5}	0.288	5×10^{-6}	4×10^{-5}	0.351	2×10^{-6}
		350	350	6×10^{-5}	0.268	6×10^{-6}	1×10^{-5}	0.319	4×10^{-6}
		1200	1200	5×10^{-5}	0.240	1×10^{-6}	3×10^{-6}	0.277	4×10^{-6}
	Reference	-	-	9×10^{-4}	0.928	7×10^{-6}	8×10^{-4}	0.758	8×10^{-7}
	Reference	-	-	4×10^{-5}	0.279	6×10^{-7}	6×10^{-5}	0.368	5×10^{-8}

the spatial qualities of the left and right views of an S3D video.

$$S_i = \frac{Spat_i^L + Spat_i^R}{2},$$

where, S_i represents the overall spatial quality score of the i^{th} frame of an S3D video, L, R represent the left and right views of an S3D video respectively. $Spat$ represents the 2D spatial quality score of the frame as computed using a state-of-the-art 2D NR IQA algorithm. Specifically, we rely on the following NR IQA algorithms for estimating the spatial quality score of the frames: Sparsity Based Image Quality Evaluator (SBIQE) [58], Blind/referenceless Image Spatial Quality Evaluator (BRISQUE) [59], Natural Image Quality Evaluator (NIQE) [60]. For brevity, we refer the reader to the respective references for descriptions of these algorithms. All these algorithms deliver state-of-the-art performance on standard IQA databases.

Fig. 5 shows the frame-wise NIQE scores of reference and H.264 distorted versions of the Boxers video sequence of IRCCYN S3D video database. The NIQE scores are clearly varying according to the quality level and is therefore a good discriminatory feature for quality prediction.

E. Supervised Learning and Quality Estimation

As mentioned previously, we used three spatial scales and six orientations in our analysis resulting in a total of 18 subbands for every stereoscopic video frame. The BGGD model parameters are computed at every subband resulting in a feature vector $f = [\alpha^1 \dots \alpha^{18}; \beta^1 \dots \beta^{18}]$ per frame. For an S3D video, the feature vector set is $[f_1, f_2 \dots f_n]$, where n is the number of video frames and $f_i = [\alpha_i^1 \dots \alpha_i^{18}; \beta_i^1 \dots \beta_i^{18}]$; $1 \leq i \leq n - 1$. The spatial quality feature (S_i) is appended to the aforementioned BGGD features to explicitly rely on spatial quality. Finally, the feature vector of a video frame is $f_i^s = [\alpha_i^1 \dots \alpha_i^{18}; \beta_i^1 \dots \beta_i^{18}; S_i]$. We believe that over short temporal durations, the average DMOS score of an S3D video and the frame-level DMOS score are highly correlated and are interchangeable. Therefore, we performed the regression of the frame-level features f_i^s and the video-level DMOS scores D as its label. For video V ,

$$f_i^{sV} = [\alpha_i^1 \dots \alpha_i^{18}; \beta_i^1 \dots \beta_i^{18}; S_i], \quad (3)$$

with the corresponding label D_V . This feature vector and label set is used to train an SVR. SVR is shown to provide good performance even when the available training set size is small,

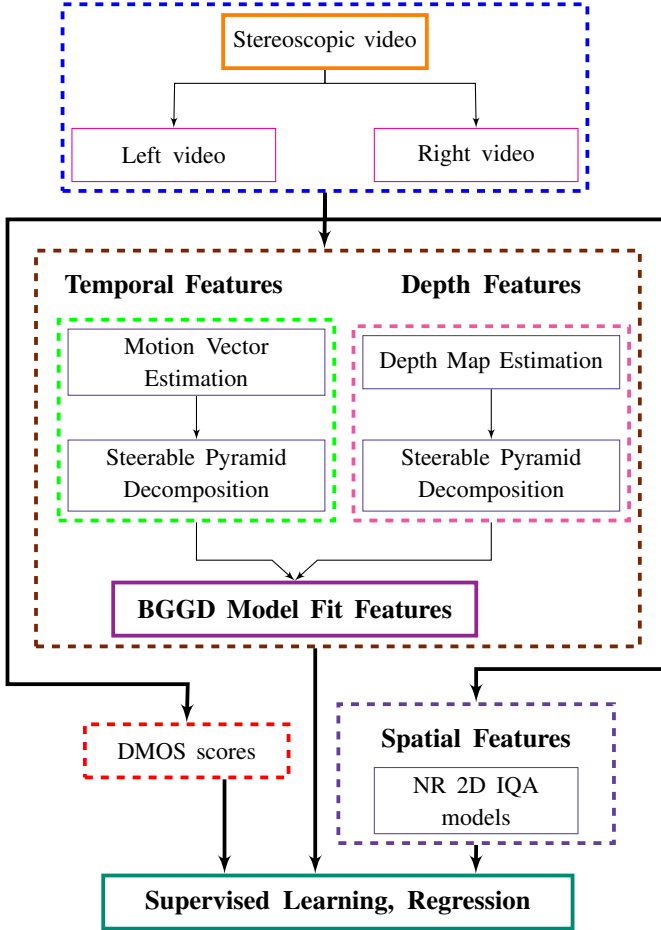


Fig. 4: Flowchart of the proposed VQUEMODES algorithm.

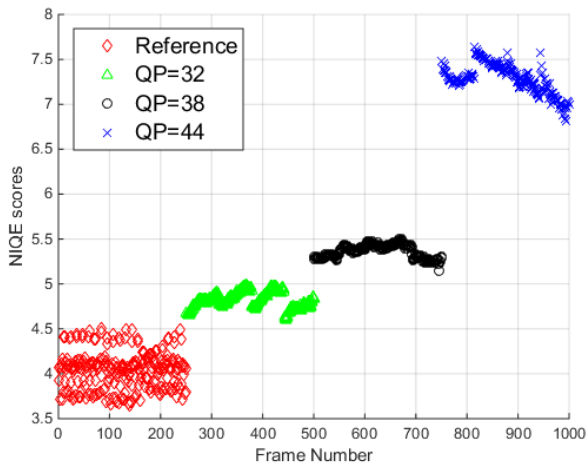


Fig. 5: Frame-wise NIQE scores of the Boxers video reference sequence and H.264 distortion versions. It is evident that quality variations are clearly tracked.

demonstrate accurate performance in one-versus-rest schemes [61], provide sparse solutions [62] and accurate estimation of global minimum [63] etc. In our work, we used the radial basis function (RBF) kernel as it gave the best overall performance.

We use regression to estimate the scores of test video frames. It should be noted that the training and regression happen at the frame-level. The overall (video-level) quality score is estimated by averaging the frame-level quality estimates.

IV. RESULTS AND DISCUSSION

While several S3D quality assessment databases have been reported in the literature, few of them are open source. We report our results on two popular publicly available databases: the IRCCYN and LFOVIA S3D VQA databases.

The IRCCYN database [48] is composed of 10 pristine and 70 distorted video sequences with a good variation in texture, motion and depth components. The video sequences are captured with Panasonic AG-3DA1E twin-lens camera and the baseline separation between lenses is 60 mm. The video sequences are either 16 seconds or 13 seconds in duration and have a resolution of 1920×1080 pixels with a frame rate of 25fps. All the video sequences are encoded in YUV420P format and saved in .avi container. This database is a combination of H.264 and JP2K compression artefact distortions. They utilized the JM reference software to add H.264 compression artefacts by varying the quantization parameter ($QP = 32, 38, 44$). JP2K artifacts (2, 8, 16, 32 Mb/s) are added on a frame-by-frame basis for both views. These compression artefacts are symmetrically applied on left and right videos. The subjective study is performed in absolute category rating with hidden reference (ACR-HR) method and they published the DMOS values as quality scores. In our evaluation, we limited our temporal extent to the first 10 seconds of the video to avoid issues with blank frames. This applies specifically to the Boxers and Soccer in the database.

The LFOVIA database [54] has H.264 compressed stereoscopic video sequences. The database has 6 pristine and 144 distorted video sequences and the videos are encoded in YUV 420P format and saved in mp4 container. The compression artifacts were introduced using *ffmpeg* by changing the bitrate (100, 200, 350, 1200 Kbps) as the quality variation parameter. The video sequences have a resolution of 1836×1056 pixels with a frame rate of 25fps and a duration of 10 sec. This database is a combination of symmetric and asymmetric stereoscopic video sequences. They also performed the subjective study in ACR-HR method and published DMOS values as quality scores. The RMIT database has 47 reference video sequences and does not have any distorted video sequences or subjective scores. Therefore, we did not perform quality assessment on this database.

For both the databases, 80% of the videos are used for SVR training and the remaining samples are used for regression. In other words, the training and test sets are obtained by partitioning the set of available videos in the 80:20 proportion. Once this video-level partitioning is done, the actual training happens at the frame-level. During regression, the frame-level scores are estimated and averaged to compute the video-level

TABLE II: 2D and 3D IQA/VQA performance evaluation on IRCCYN and LFOVIA S3D video databases. **Bold names** indicate NR QA methods.

Algorithm	IRCCYN Database			LFOVIA Database		
	LCC	SROCC	RMSE	LCC	SROCC	RMSE
SSIM [64]	0.6359	0.2465	1.0264	0.8816	0.8828	6.1104
MS-SSIM [65]	0.9100	0.8534	0.6512	0.8172	0.7888	8.9467
SBIQE [58]	0.0081	0.0054	1.2712	0.0010	0.0043	16.0311
BRISQUE [59]	0.7535	0.8145	0.6535	0.6182	0.6000	12.6001
NIQE [60]	0.5729	0.5664	0.8464	0.7206	0.7376	11.1138
STMAD [66]	0.6400	0.3495	0.9518	0.6802	0.6014	9.4918
FLOSIM [55]	0.9178	0.9111	0.4918	-	-	-
Chen <i>et al.</i> [49]	0.7886	0.7861	0.7464	0.8573	0.8588	6.6655
STRIQE [25]	0.7931	0.6400	0.7544	0.7543	0.7485	8.5011
VQUEMODES (NIQE)	0.9697	0.9637	0.2635	0.8943	0.8890	5.9124

TABLE III: 2D and 3D IQA/VQA performance evaluation on different distortions of IRCCYN S3D video database. **Bold names** indicate NR QA methods.

Algorithm	H.264			JP2K		
	LCC	SROCC	RMSE	LCC	SROCC	RMSE
SSIM [64]	0.7674	0.5464	0.8843	0.7283	0.5974	0.9202
MS-SSIM [65]	0.8795	0.6673	0.6955	0.9414	0.9299	0.4327
SBIQE [58]	0.0062	0.0058	1.9856	0.0120	0.0574	1.0289
BRISQUE [59]	0.7915	0.7637	0.7912	0.8048	0.8999	0.5687
NIQE [60]	0.6814	0.6412	0.8715	0.6558	0.6427	0.7157
STMAD [66]	0.7641	0.7354	0.7296	0.8388	0.7236	0.7136
FLOSIM [55]	0.9265	0.8987	0.4256	0.9665	0.9495	0.3359
Chen <i>et al.</i> [49]	0.6618	0.5720	0.6915	0.8723	0.8724	0.6182
STRIQE [25]	0.7430	0.7167	0.8433	0.8403	0.8175	0.5666
VQUEMODES (NIQE)	0.9594	0.9439	0.1791	0.9859	0.9666	0.0912

TABLE IV: 2D and 3D IQA/VQA performance evaluation on symmetric and asymmetric stereoscopic videos of LFOVIA S3D video database. **Bold names** indicate NR QA methods.

Algorithm	Symm			Asymm		
	LCC	SROCC	RMSE	LCC	SROCC	RMSE
SSIM [64]	0.9037	0.8991	7.0246	0.8769	0.8755	5.8162
MS-SSIM [65]	0.8901	0.8681	21.2322	0.8423	0.7785	15.1681
SBIQE [58]	0.0006	0.0027	25.4484	0.0021	0.0051	12.0123
BRISQUE [59]	0.7829	0.7859	15.8298	0.5411	0.5303	10.1719
NIQE [60]	0.8499	0.8705	13.4076	0.6835	0.6929	8.8334
STMAD [66]	0.7815	0.8000	10.2358	0.6534	0.6010	9.1614
Chen <i>et al.</i> [49]	0.9435	0.9182	5.4346	0.8370	0.8376	6.6218
STRIQE [25]	0.8275	0.8017	9.2105	0.7559	0.7492	7.9321
VQUEMODES (NIQE)	0.9285	0.9236	3.9852	0.8955	0.8490	6.9563

TABLE V: Performance evaluation on IRCCYN S3D video database with different 2D NR IQA models in proposed algorithm.

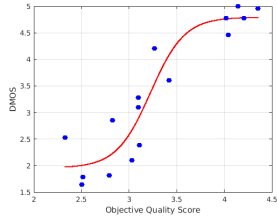
	Algorithm	H.264			JP2K			Overall		
		LCC	SROCC	RMSE	LCC	SROCC	RMSE	LCC	SROCC	RMSE
VQUEMODES	SBIQE [58]	0.9262	0.8956	0.3286	0.9706	0.9473	0.2415	0.9622	0.9377	0.3039
	BRISQUE [59]	0.9517	0.9323	0.2319	0.9809	0.9577	0.1097	0.9624	0.9482	0.3019
	NIQE [60]	0.9594	0.9439	0.1791	0.9859	0.9666	0.0912	0.9697	0.9637	0.2635

TABLE VI: Performance evaluation on LFOVIA S3D video database with different 2D NR IQA models in proposed algorithm.

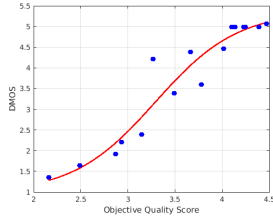
	Algorithm	Symm			Asymm			Overall		
		LCC	SROCC	RMSE	LCC	SROCC	RMSE	LCC	SROCC	RMSE
VQUEMODES	SBIQE [58]	0.9000	0.8913	4.5900	0.8532	0.8234	7.1376	0.8483	0.8341	7.3476
	BRISQUE [59]	0.9125	0.9013	4.3980	0.8792	0.8489	6.8563	0.8827	0.8693	5.9859
	NIQE [60]	0.9285	0.9236	3.9852	0.8955	0.8490	6.9563	0.8943	0.8890	5.9124

TABLE VII: Performance comparison with different 3D VQA metrics on IRCCYN S3D video database. **Bold names** indicate NR QA methods.

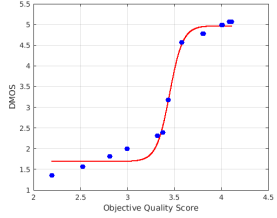
Algorithm	H.264			JP2K			Overall		
	LCC	SROCC	RMSE	LCC	SROCC	RMSE	LCC	SROCC	RMSE
Temporal FLOSIM [55]	0.6453	0.5489	0.6958	0.8441	0.8278	0.7027	0.7252	0.7097	0.8528
VQUEMODES (no spatial)	0.9253	0.8955	0.3555	0.9690	0.9477	0.2572	0.9569	0.9330	0.3162
PQM [10]	-	-	-	-	-	-	0.6340	0.6006	0.8784
Chen _{3D} [11]	0.7963	0.8035	2.5835	0.9358	0.8884	3.2863	0.8227	0.8201	2.9763
STRIQE _{3D} [11]	0.6836	0.6263	2.3683	0.8778	0.8513	3.2121	0.7599	0.7525	2.8374
FLOSIM _{3D} [11]	0.9589	0.9478	0.3863	0.9738	0.9548	0.2976	0.9178	0.9111	0.4918
PHVS-3D [30]	-	-	-	-	-	-	0.5480	0.5146	0.9501
3D-STIS [31]	-	-	-	-	-	-	0.6417	0.6214	0.9067
SJND-SVA [32]	0.5834	0.6810	0.6672	0.8062	0.6901	0.5079	0.6503	0.6229	0.8629
Yang <i>et al.</i> [45]	-	-	-	-	-	-	0.8949	0.8552	0.4929
BSVQE [46]	0.9168	0.8857	-	0.8953	0.8383	-	0.9239	0.9086	-
VQUEMODES (NIQE)	0.9594	0.9439	0.1791	0.9859	0.9666	0.0912	0.9697	0.9637	0.2635



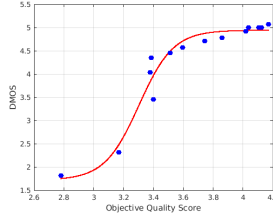
(a) VQUEMODES (no spatial).



(b) VQUEMODES (SBIQE).



(c) VQUEMODES (BRISQUE).

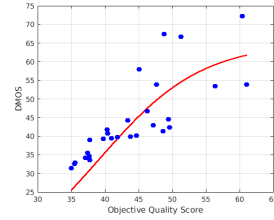


(d) VQUEMODES (NIQE).

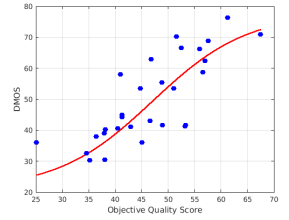
Fig. 6: Scatter plots of proposed VQUEMODES algorithm prediction without and with different spatial metrics (SBIQE/BRISQUE/NIQE) versus DMOS values on the IRCCYN database.

quality score. We empirically justify the averaging of the frame-level scores to generate the video-level score. In over 1000 regression iterations, we found that the standard deviation of frame-level scores for a given video varied between 0.2×10^{-8} and 0.25. This observation, combined with the high correlation of the average scores with DMOS values shown in Tables II - VII provide evidence for the effectiveness of our approach.

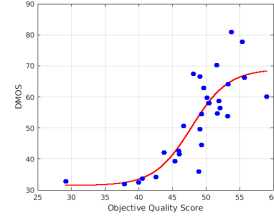
We used the open-source SVM package *LIBSVM* [67] in our experiments. We performed the training and testing 1000 times for statistical consistency with a random assignment of video-level samples without overlap between the training and testing sets. The reported results are the average over these 1000 trials. The performance of the proposed metric is measured using the following statistical measures: Linear Correlation Coefficient (LCC), Spearman's Rank Order Correlation Coefficient (SROCC) and Root Mean Square Error (RMSE). LCC signifies the linear dependence between two variables and SROCC reveals the monotonic relationship between two quantities.



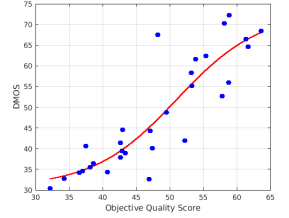
(a) VQUEMODES (no spatial).



(b) VQUEMODES (SBIQE).



(c) VQUEMODES (BRISQUE).



(d) VQUEMODES (NIQE).

Fig. 7: Scatter plots of proposed VQUEMODES algorithm prediction without and with different spatial metrics (SBIQE/BRISQUE/NIQE) versus DMOS values on the LFOVIA database.

Higher LCC and SROCC value point to a good agreement between the subjective and objective. RMSE quantifies the magnitude of the error between estimated quality scores and DMOS values. All these results are evaluated after performing a non-linear logistic fit. We followed the standard procedure recommended by Video Quality Experts Group (VQEG) [68] to perform the non-linear regression with 4-parameter logistic transform given by

$$f(x) = \frac{\tau_1 - \tau_2}{1 + \exp\left(\frac{x - \tau_3}{\tau_4}\right)} + \tau_2,$$

where x denotes the raw objective score, and τ_1, τ_2, τ_3 and τ_4 are the free parameters selected to provide the best fit of the predicted scores to the DMOS values.

Table II shows the performance of the proposed metric VQUEMODES (NIQE) on the IRCCYN and LFOVIA databases. We used the NIQE scores as spatial quality score in the proposed algorithm. Also, we compared our metric's performance with different state-of-art 2D IQA/VQA and 3D IQA/VQA models. SSIM [64], MS-SSIM [65] are FR 2D IQA

metrics and SBIQE [58], NIQE [60] and BRISQUE [59] are 2D NR IQA metrics. These IQA metrics were applied on a frame-by-frame basis for each view and the final quality is computed by calculating the average of frame scores of both views. STMAD [66] and FLOSIM [55] are 2D FR VQA metrics applied on individual views and the final score is computed by calculating the mean of both view scores. Chen *et al.* [49] and STRIQE [25] are stereoscopic FR IQA metrics. These metrics were applied on a frame-by-frame basis for the 3D video and the final quality score is computed by calculating the mean of the frame-level quality scores. From the table it is clear that the proposed metric outperforms all of the 2D IQA/VQA and 3D IQA models.

Table III shows the proposed metric's evaluation on different distortions of the IRCCYN database. Table IV shows the performance evaluation of proposed metric on symmetric and asymmetric S3D video sequences of the LFOVIA database. Symmetric stereoscopic video has both views at same quality and asymmetric stereoscopic video has each view at a different quality. From these results it is clear that the proposed metric has state-of-art performance compared to the other quality metrics in both cases of different distortions (H.264 and JP2K) and symmetric and asymmetric distorted stereoscopic video sequences.

We checked the efficacy of proposed algorithm by replacing the NIQE scores with other popular 2D NR IQA methods as well. Tables V and VI shows the performance evaluation of proposed metric VQUEMODES on the IRCCYN and LFOVIA databases respectively. From these results it is clear that the proposed metric demonstrates consistent and state-of-art results across spatial metrics and across distortion types. Table VII shows the performance comparison of the proposed method with different 3D VQA metrics on IRCCYN database. PQM [10], $FLOSIM_{3D}$ [11], PHVS-3D [30], 3D-STs [31] and SJND-SVQ [32] are S3D FR VQA models. Temporal FLOSIM is a part of the FLOSIM [55] metric which computes the quality score of a video based on disturbances in motion components. $Chen_{3D}$ and $STRIQE_{3D}$ are 3D FR VQA metrics and these models are extensions of the Chen *et al.* and STRIQE (3D IQA metrics) by including the motion scores computed by Temporal FLOSIM. Yang *et al.* and BSVQE [46] are S3D NR VQA models.

To highlight the effectiveness of using joint motion and depth statistics for NR VQA, we report the performance of VQUEMODES without including the spatial quality feature in Table VII. The corresponding scatter plot for this case is shown in Fig. 6. It is clear from these numbers and plots that our proposed statistical features are indeed very effective for S3D NR VQA. It is also clear that the combination of joint motion and depth statistical features and spatial quality features (NIQE) has shown a small but consistent performance improvement (compared to the stand-alone motion and depth features) indicating that spatial quality does play a role in S3D VQA. Figs. 6 and 7 shows the scatter plots of proposed algorithm with different spatial metrics on the IRCCYN and LFOVIA S3D databases respectively. These scatter plots also provide corroborative evidence for the small but important role played by the spatial feature in improving overall NR VQA

performance.

V. CONCLUSIONS AND FUTURE WORK

Inspired by the neurophysical response of the MT area to motion and depth inputs, we proposed a BGGD model to capture the joint statistical dependencies between motion and disparity subband coefficients of natural S3D videos. The utility and efficacy of the proposed BGGD model was demonstrated in an NR stereo VQA application dubbed VQUEMODES. VQUEMODES was evaluated on the IRCCYN, LFOVIA S3D video databases and shown to have state-of-the-art performance compared to the other 2D and 3D IQA/VQA metrics. We believe that the proposed model could be useful in several applications like depth frame estimation from temporal feature maps, visual navigation, denoising, quality assessment etc.

REFERENCES

- [1] Motion Picture Association of America, "Theatrical market statistics 2013," 2015.
- [2] "3D Technology Statista Dossier, <https://www.statista.com/study/16305/3d-technology-statista-dossier/>."
- [3] P. Merkle, K. Miller, and T. Wiegand, "3d video: acquisition, coding, and display," *IEEE Transactions on Consumer Electronics*, vol. 56, pp. 946–950, May 2010.
- [4] S. P. Yasakethu, W. Fernando, B. Kamolrat, and A. Kondo, "Analyzing perceptual attributes of 3D video," *IEEE Transactions on Consumer Electronics*, vol. 55, no. 2, pp. 864–872, 2009.
- [5] C. T. E. R. Hewage, S. T. Worrall, S. Dogan, S. Villette, and A. M. Kondo, "Quality evaluation of color plus depth map-based stereoscopic video," *IEEE Journal of Selected Topics in Signal Processing*, vol. 3, pp. 304–318, April 2009.
- [6] C. D. M. Regis, J. V. de Miranda Cardoso, Í. de Pontes Oliveira, and M. S. de Alencar, "Objective estimation of 3D video quality: A disparity-based weighting strategy," in *IEEE International Symposium on Broadband Multimedia Systems and Broadcasting*, pp. 1–6, 2013.
- [7] E. Bosc, R. Pepion, P. Le Callet, M. Koppel, P. Ndjiki-Nya, M. Presigout, and L. Morin, "Towards a new quality metric for 3D synthesized view assessment," *IEEE Journal of Selected Topics in Signal Processing*, vol. 5, no. 7, pp. 1332–1343, 2011.
- [8] A. Banitalebi-Dehkordi, M. T. Pourazad, and P. Nasiopoulos, "An efficient human visual system based quality metric for 3d video," *Multimedia Tools and Applications*, vol. 75, no. 8, pp. 4187–4215, 2016.
- [9] F. Battisti, M. Carli, A. Stramacci, A. Boev, and A. Gotchev, "A perceptual quality metric for high-definition stereoscopic 3D video," in *Proc. SPIE*, vol. 9399, 2015.
- [10] P. Joveluro, H. Malekmohamadi, W. A. C. Fernando, and A. M. Kondo, "Perceptual video quality metric for 3D video quality assessment," in *3DTV-Conference: The True Vision - Capture, Transmission and Display of 3D Video*, pp. 1–4, June 2010.
- [11] B. Appina, M. K., and S. S. Channappayya, "A full reference stereoscopic video quality assessment metric," in *IEEE International Conference on Acoustics, Speech and Signal Processing (ICASSP)*, pp. 2012–2016, March 2017.
- [12] J. H. Maunsell and D. C. Van Essen, "Functional properties of neurons in middle temporal visual area of the macaque monkey. i. selectivity for stimulus direction, speed, and orientation," *Journal of Neurophysiology*, vol. 49, no. 5, pp. 1127–1147, 1983.
- [13] J.-P. Roy, H. Komatsu, and R. H. Wurtz, "Disparity sensitivity of neurons in monkey extrastriate area mst," *The Journal of Neuroscience*, vol. 12, no. 7, pp. 2478–2492, 1992.
- [14] G. C. DeAngelis and W. T. Newsome, "Organization of disparity-selective neurons in macaque area mt," *The Journal of Neuroscience*, vol. 19, no. 4, pp. 1398–1415, 1999.
- [15] P. Dayan and L. Abbott, "Theoretical neuroscience: computational and mathematical modeling of neural systems," *Journal of Cognitive Neuroscience*, vol. 15, no. 1, pp. 154–155, 2003.
- [16] E. P. Simoncelli and B. A. Olshausen, "Natural image statistics and neural representation," *Annual review of Neuroscience*, vol. 24, no. 1, pp. 1193–1216, 2001.

- [17] J. Huang, A. Lee, and D. Mumford, "Statistics of range images," in *IEEE Conference on Computer Vision and Pattern Recognition*, vol. 1, pp. 324–331 vol.1, 2000.
- [18] Y. Liu, A. C. Bovik, and L. K. Cormack, "Disparity statistics in natural scenes," *Journal of Vision*, vol. 8, no. 11, p. 19, 2008.
- [19] Y. Liu, L. K. Cormack, and A. C. Bovik, "Dichotomy between luminance and disparity features at binocular fixations," *Journal of Vision*, vol. 10, no. 12, pp. 23–23, 2010.
- [20] B. Potetz and T. S. Lee, "Statistical correlations between two-dimensional images and three-dimensional structures in natural scenes," *JOSA A*, vol. 20, no. 7, pp. 1292–1303, 2003.
- [21] Y. Liu, L. K. Cormack, and A. C. Bovik, "Statistical modeling of 3-d natural scenes with application to bayesian stereopsis," *IEEE Transactions on Image Processing*, vol. 20, pp. 2515–2530, Sept 2011.
- [22] Y. Liu, L. K. Cormack, and A. C. Bovik, "Luminance, disparity, and range statistics in 3d natural scenes," in *IS&T/SPIE Electronic Imaging*, pp. 72401G–72401G, International Society for Optics and Photonics, 2009.
- [23] C. C. Su, A. C. Bovik, and L. K. Cormack, "Natural scene statistics of color and range," in *IEEE International Conference on Image Processing*, pp. 257–260, Sept 2011.
- [24] M. J. Chen, L. K. Cormack, and A. C. Bovik, "No-reference quality assessment of natural stereopairs," *IEEE Transactions on Image Processing*, vol. 22, pp. 3379–3391, Sept 2013.
- [25] S. Khan Md, B. Appina, and S. Channappayya, "Full-reference stereo image quality assessment using natural stereo scene statistics," *IEEE Signal Processing Letters*, vol. 22, pp. 1985–1989, Nov 2015.
- [26] C. C. Su, L. K. Cormack, and A. C. Bovik, "Oriented correlation models of distorted natural images with application to natural stereopair quality evaluation," *IEEE Transactions on Image Processing*, vol. 24, pp. 1685–1699, May 2015.
- [27] B. Appina, S. Khan, and S. S. Channappayya, "No-reference stereoscopic image quality assessment using natural scene statistics," *Signal Processing: Image Communication*, vol. 43, pp. 1–14, 2016.
- [28] W. Hachicha, M. Kaaniche, A. Beghdadi, and F. Cheikh, "No-reference stereo image quality assessment based on joint wavelet decomposition and statistical models," *Signal Processing: Image Communication*, vol. 54, pp. 107–117, 2017.
- [29] A. Mittal, A. K. Moorthy, J. Ghosh, and A. C. Bovik, "Algorithmic assessment of 3D quality of experience for images and videos," in *Digital Signal Processing Workshop and IEEE Signal Processing Education Workshop (DSP/SPE)*, pp. 338–343, 2011.
- [30] L. Jin, A. Gotchev, A. Boev, and K. Egiazarian, "Validation of a new full reference metric for quality assessment of mobile 3d tv content," in *Signal Processing Conference, 2011 19th European*, pp. 1894–1898, Aug 2011.
- [31] J. Han, T. Jiang, and S. Ma, "Stereoscopic video quality assessment model based on spatial-temporal structural information," in *Visual Communications and Image Processing (VCIP), 2012 IEEE*, pp. 1–6, Nov 2012.
- [32] F. Qi, D. Zhao, X. Fan, and T. Jiang, "Stereoscopic video quality assessment based on visual attention and just-noticeable difference models," *Signal, Image and Video Processing*, vol. 10, no. 4, pp. 737–744, 2016.
- [33] D. V. S. De Silva, W. A. C. Fernando, G. Nur, E. Ekmekcioglu, and S. T. Worrall, "3D video assessment with just noticeable difference in depth evaluation," in *IEEE International Conference on Image Processing*, pp. 4013–4016, 2010.
- [34] C. Galkandage, J. Calic, S. Dogan, and J.-Y. Guillemot, "Stereoscopic video quality assessment using binocular energy," *IEEE Journal of Selected Topics in Signal Processing*, 2016.
- [35] V. De Silva, H. K. Arachchi, E. Ekmekcioglu, and A. Kondoz, "Toward an impairment metric for stereoscopic video: A full-reference video quality metric to assess compressed stereoscopic video," *IEEE transactions on image processing*, vol. 22, no. 9, pp. 3392–3404, 2013.
- [36] C. T. Hewage and M. G. Martini, "Reduced-reference quality assessment for 3D video compression and transmission," *IEEE Transactions on Consumer Electronics*, vol. 57, no. 3, pp. 1185–1193, 2011.
- [37] M. Yu, K. Zheng, G. Jiang, F. Shao, and Z. Peng, "Binocular perception based reduced-reference stereo video quality assessment method," *Journal of Visual Communication and Image Representation*, vol. 38, pp. 246–255, 2016.
- [38] Z. P. Sazzad, S. Yamanaka, and Y. Horita, "Spatio-temporal segmentation based continuous no-reference stereoscopic video quality prediction," in *IEEE International Workshop on Quality of Multimedia Experience*, pp. 106–111, 2010.
- [39] K. Ha and M. Kim, "A perceptual quality assessment metric using temporal complexity and disparity information for stereoscopic video," in *IEEE International Conference on Image Processing*, pp. 2525–2528, 2011.
- [40] M. Solh and G. AlRegib, "A no-reference quality measure for dibr-based 3D videos," in *IEEE International Conference on Multimedia and Expo*, pp. 1–6, 2011.
- [41] M. M. Hasan, J. F. Arnold, and M. R. Frater, "No-reference quality assessment of 3D videos based on human visual perception," in *IEEE International Conference on 3D Imaging*, pp. 1–6, 2014.
- [42] A. R. Silva, M. E. V. Melgar, and M. C. Farias, "A no-reference stereoscopic quality metric," in *Proc. SPIE*, vol. 9393, 2015.
- [43] Y. Han, Z. Yuan, and G.-M. Muntean, "Extended no reference objective quality metric for stereoscopic 3D video," in *IEEE International Conference on Communication Workshop*, pp. 1729–1734, 2015.
- [44] S. A. Mahmood and R. F. Ghani, "Objective quality assessment of 3D stereoscopic video based on motion vectors and depth map features," in *IEEE Computer Science and Electronic Engineering Conference*, pp. 179–183, 2015.
- [45] J. Yang, H. Wang, W. Lu, B. Li, A. Badiid, and Q. Meng, "A no-reference optical flow-based quality evaluator for stereoscopic videos in curvelet domain," *Information Sciences*, vol. 414, pp. 133–146, 2017.
- [46] Z. Chen, W. Zhou, and W. Li, "Blind stereoscopic video quality assessment: From depth perception to overall experience," *IEEE Transactions on Image Processing*, 2017.
- [47] F. Pascal, L. Bombrun, J.-Y. Tourneret, and Y. Berthoumieu, "Parameter estimation for multivariate generalized gaussian distributions," *IEEE Transactions on Signal Processing*, vol. 61, no. 23, pp. 5960–5971, 2013.
- [48] M. Urvoy, M. Barkowsky, R. Cousseau, Y. Koudota, V. Ricorde, P. L. Callet, J. Gutierrez, and N. Garca, "Nama3ds1-cospad1: Subjective video quality assessment database on coding conditions introducing freely available high quality 3D stereoscopic sequences," in *International Workshop on Quality of Multimedia Experience*, pp. 109–114, July 2012.
- [49] M.-J. Chen, C.-C. Su, D.-K. Kwon, L. K. Cormack, and A. C. Bovik, "Full-reference quality assessment of stereopairs accounting for rivalry," *Signal Processing: Image Communication*, vol. 28, no. 9, pp. 1143–1155, 2013.
- [50] M. J. Black and P. Anandan, "A framework for the robust estimation of optical flow," in *IEEE International Conference on Computer Vision*, pp. 231–236, 1993.
- [51] M. Jakubowski and G. Pastuszak, "Block-based motion estimation algorithms survey," *Opto-Electronics Review, Springer*, vol. 21, no. 1, pp. 86–102, 2013.
- [52] R. A. Young, "The gaussian derivative model for spatial vision: I. retinal mechanisms," *Spatial vision*, vol. 2, no. 4, pp. 273–293, 1987.
- [53] E. Cheng, P. Burton, J. Burton, A. Joseski, and I. Burnett, "RMIT3DV: Pre-announcement of a creative commons uncompressed HD 3D video database," in *IEEE International Workshop on Quality of Multimedia Experience*, pp. 212–217, 2012.
- [54] B. Appina, M. K., and S. S. Channappayya, "Subjective and objective study of the relation between 3D and 2D views based on depth and bitrate," in *IS&T/SPIE, Electronic Imaging*, pp. 145–150, January 2017.
- [55] M. K. and S. S. Channappayya, "An optical flow-based full reference video quality assessment algorithm," *IEEE Transactions on Image Processing*, vol. 25, pp. 2480–2492, June 2016.
- [56] W. J. Levelt, *On binocular rivalry*, vol. 2. Mouton The Hague, 1968.
- [57] D. H. Hubel and T. N. Wiesel, "Receptive fields and functional architecture in two nonstriate visual areas (18 and 19) of the cat," *Journal of Neurophysiology*, vol. 28, no. 2, pp. 229–289, 1965.
- [58] K. V. S. N. L. M. Priya and S. S. Channappayya, "A novel sparsity-inspired blind image quality assessment algorithm," in *IEEE Global Conference on Signal and Information Processing*, pp. 984–988, Dec 2014.
- [59] A. Mittal, A. K. Moorthy, and A. C. Bovik, "No-reference image quality assessment in the spatial domain," *IEEE Transactions on Image Processing*, vol. 21, no. 12, pp. 4695–4708, 2012.
- [60] A. Mittal, R. Soundararajan, and A. C. Bovik, "Making a completely blind image quality analyzer," *IEEE Signal Processing Letters*, vol. 20, no. 3, pp. 209–212, 2013.
- [61] R. Rifkin and A. Klautau, "In defense of one-vs-all classification," *The Journal of Machine Learning Research*, vol. 5, pp. 101–141, 2004.
- [62] B. Schölkopf, K.-K. Sung, C. J. Burges, F. Girosi, P. Niyogi, T. Poggio, and V. Vapnik, "Comparing support vector machines with gaussian kernels to radial basis function classifiers," *IEEE Transactions on Signal Processing*, vol. 45, no. 11, pp. 2758–2765, 1997.

- [63] N. Cristianini and J. Shawe-Taylor, *An introduction to support vector machines and other kernel-based learning methods*. Cambridge University press, 2000.
- [64] Z. Wang, A. C. Bovik, H. R. Sheikh, and E. P. Simoncelli, "Image quality assessment: from error visibility to structural similarity," *IEEE Transactions on Image Processing*, vol. 13, pp. 600–612, April 2004.
- [65] Z. Wang, E. P. Simoncelli, and A. C. Bovik, "Multiscale structural similarity for image quality assessment," in *IEEE Asilomar Conference on Signals, Systems Computers*, vol. 2, pp. 1398–1402 Vol.2, Nov 2003.
- [66] P. V. Vu, C. T. Vu, and D. M. Chandler, "A spatiotemporal most-apparent-distortion model for video quality assessment," in *IEEE International Conference on Image Processing*, pp. 2505–2508, 2011.
- [67] C.-C. Chang and C.-J. Lin, "Libsvm: a library for support vector machines," *ACM Transactions on Intelligent Systems and Technology (TIST)*, vol. 2, no. 3, p. 27, 2011.
- [68] "Vqeg. (aug. 2003). final report from the video quality experts group on the validation of objective models of video quality assessment, phase ii. [online]. available: <http://www.its.bldrdoc.gov/vqeg/projects/frtv-phase-ii/frtv-phase-ii.aspx>."